18th World Conference on Nondestructive Testing, 16-20 April 2012, Durban, South Africa

Real-Time Inspection of Complex Composite Structures with a Self-Adaptive Ultrasonic Technique

Sébastien ROBERT[1], Olivier CASULA[1], Olivier ROY[2], Guillaume NEAU[2]

[1]CEA-LIST, F-91191, Gif-sur-Yvette cedex, France
sebastien.robert@cea.fr, olivier.casula@cea.fr

[2]M2M, 1 rue de Terre-Neuve, 91940, Les Ulis, France
o.roy@m2m-ndt.com, g.neau@m2m-ndt.com

Abstract
In aircraft industry, composite structures under testing have complex and variable geometries. In these cases, an optimal use of ultrasonic phased-array requires specific algorithms in electronic systems in order to achieve rapid and reliable inspections. To fulfil such requirements, a new real-time adaptive inspection method is presented. This technique enables the transmission of an incident wave-front parallel to any complex surface. It allows to inspect one given component presenting variable geometries in its totality using a same transducer array. This is achieved by means of an iterative algorithm that does not require the knowledge of the geometrical and acoustical properties of the component undergoing inspection. In this paper, the real-time adaptive process is illustrated through measurements obtained with different typical aircraft composite structures.

Keywords: Ultrasonic Testing, Phased Array, Aerospace, Carbon Fiber Composite

1. Introduction

New commercial aircrafts incorporate more and more composite materials in their structures to ensure both lightness and robustness. This increase in composite surfaces motivates the development of new technologies and algorithms in ultrasonic non-destructive testing (NDT) to achieve fast and reliable inspections.
Ultrasonic phased arrays represent the most promising technological solution to reduce scanning times and to also improve the characterization of defects. In general, these sensors are used to detect manufacturing defects (porosities, foreign bodies, delaminations, cracks...) introduced in composite materials during manufacturing processes [1]. Inspection is performed in a tank filled with water, and a maximum scanning speed is desired to reduce NDT costs, especially for large composite structures.
One of the most famous acquisition modes is the so-called ‘paintbrush’ acquisition. It consists in transmitting once with all elements of a phased array, without delay law, and receiving elementary signals in parallel on all elements [2,3]. This mode leads to high scanning speeds that do not depend on the number of used elements. In order to improve the signal to noise ratio as well as the spatial resolution, a sub-aperture of few consecutive elements can be used in reception. This sub-aperture is electronically moved all along the total aperture to obtain a moving average of the elementary signals.
For complex composite parts, such as the corner of a stiffened part, a solution consists in using shaped probes, such as cylindrical phased arrays. The probe is placed over the convex surface and its curvature radius ensures a normal incidence transmission of the ultrasonic field at any point of the corner surface [4]. Inspection is performed by mechanically adjusting the lateral position during scanning to master the normal incidence transmission. Curved phased arrays can also include a shoe and mechanisms to compensate a misalignment between the probe and the corner radius and to also take into account curvature radius variations [5]. The

main drawback of shaped probes is that they are valid for one geometry type. Other parts of a given component (with flat, concave, shoulder geometries,...) may require a large inventory of probes with different shapes, which leads to expensive NDT costs and reduces inspection speeds when a complex component must be inspected in its entire totality.
In this paper, a new real-time adaptive inspection method is presented. The technique allows to master a normal incidence transmission through various complex surfaces using a conventional no-shaped phased array (typically a linear or matrix array with a flat active aperture). One given component presenting variable geometries can be inspected in its totality using a same probe. This is achieved by means of an iterative algorithm that is a generalization of that described in [2] and suggested in [6,7]. The basic principle consists in measuring times of flight from a surface echo recorded in paintbrush mode and in deducing an adaptive delay law generating an incident wave front parallel to the surface [8,9]. The self-adaptive technique is called SAUL method ('Surface Adaptive ULtrasounds') and has been implemented in the MultiX systems, designed by the M2M Company. The real-time processing is illustrated in the paper through acquisitions performed with different composite structures.

2. Paintbrush acquisition and principle of adaptation to complex surfaces

A corner radius of Carbon Fiber Reinforced Plastic (CFRP) is schematized in Fig. 1a. Its thickness is about 5 mm. A linear phased array with a centre frequency of 5 MHz is placed over the convex surface, with a water path of 16 mm. The probe is composed of 42 elements of 0.5x8 mm², with 0.6 mm pitch. The curvature radius of the front interface is 14 mm.

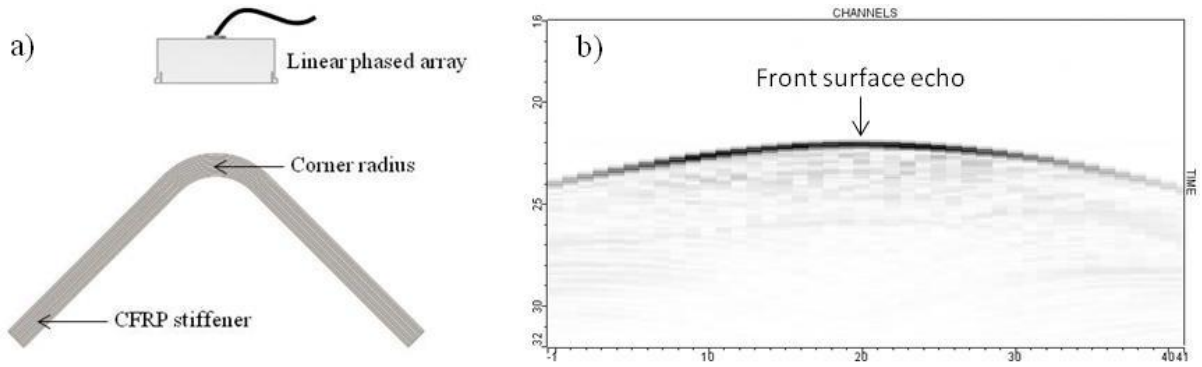

Figure 1: Experimental set-up (a) and typical B-scan obtained in paintbrush acquisition mode (b).

Basically, the paintbrush acquisition mode consists in transmitting a plane wave with the full array and recording elementary signals in parallel with all elements. The B-scan obtained is displayed in Fig. 1b. As the exited wave is not normally incident on the surface, the consecutive plies inside the material (each ply being approximately parallel to the surface) deviate the transmitted field during its propagation. This results in a poor image where both the plies and the back interface of the corner cannot be identified.
The incident wave can be partially adapted to the surface according to the processing described in [2,6,7]. First, it consists in measuring the times of flight between all elements of the array and the surface (for instance, by detecting the maxima of the surface echo envelope). Next, these times of flight are used to extract a delay law that will be applied to a second transmission. Noting t_i the time of flight between element i and the surface ($1 \leq i \leq 42$), the emission delay applied to this element is defined as:

$$E_i = \frac{1}{2}\left[\mathrm{Max}\left(t_i\right) - t_i \right]. \quad (1)$$

A reception delay law can also be applied in order to synchronize received elementary signals and, for instance, to create several coherent summations of signals using an electronic scanning of a sub-aperture. The reception delay applied to element *i* is deduced from the emission delays as follows:

$$R_i = \mathrm{Max}\left(E_i\right) - E_i \ . \tag{2}$$

The times of flight measured from the corner surface echo in Fig. 1b and the corresponding delay laws are shown below.

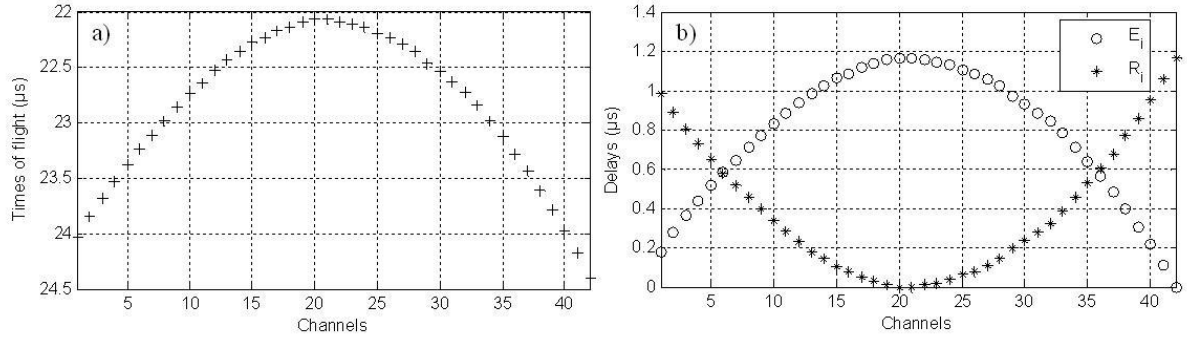

Figure 2: Times of flight measured from the front surface echo (a) and associated delay laws (b).

By applying both emission and reception delay laws to a second paintbrush acquisition, the following B-scan is obtained.

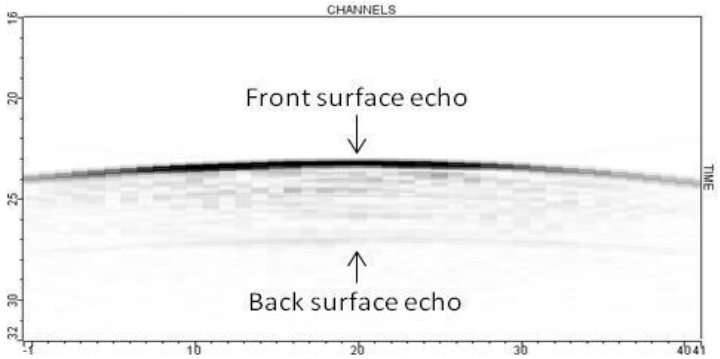

Figure 3: Paintbrush acquisition using adaptive delay laws.

Compared to the first acquisition, the back surface echo now can be identified in Fig. 3, which confirms that the delay law calculated with Eq. 1 is a good way to generate an incident wave with a wave front almost parallel to the front surface. The anisotropy effects due to the fibrous nature of the material are minimized by forcing a normal incidence transmission. However, as the incident wave is not completely adapted to the front surface, the back surface echo has a low amplitude level and the internal composite structure still cannot be identified (plies are not clearly visible). In addition, elementary signals are not exactly synchronized, which could result in a poor image if an electronic scanning with a sub-aperture of several elements was used at reception.

For a geometry as complex as a corner radius, the incident wave is not perfectly adapted to the surface since the times of flight used in the delay law computation are not specular (a specular time of flight corresponds to the path along the ray passing through the center an element and normal to the surface). A technique for measuring these specular times of flight

consists in using an electronic scanning at emission with a sub-aperture and a scanning step of 1 element. This adaptive technique is illustrated in Fig. 4 through results obtained with the same experimental set-up.

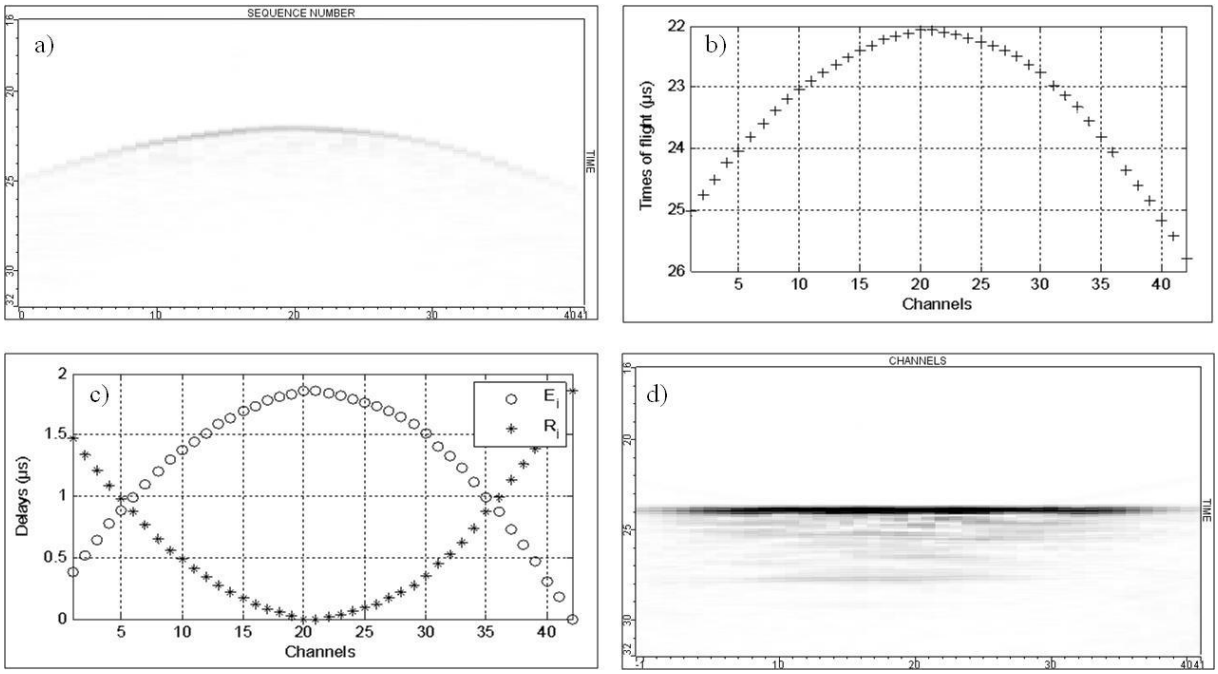

Figure 4: Adaptive process using an electronic scanning at emission: acquisition of the electronic B-scan (a); measurement of the specular times of flight (b); calculation of the emission and reception delay laws (c); transmission with all elements by applying these delay laws (d).

The electronic B-scan displayed in Fig. 4a is obtained by exiting all elements one by one, which represents a cycle of 42 transmissions. At each transmission, the same element is used as transmitter and receiver. The times of flight are measured (Fig. 4b) and used in Eqs. (1) and (2) to calculate the transmission and reception delay laws (Fig. 4c). The last step consists in transmitting once with all elements by applying these delay laws. In Fig. 4d, the elementary signals now are time coherent (the front surface echo is horizontal), which means that the incident wave is ideally adapted to the geometry. Ply echoes now can be observed.
This method thus provides the optimal delay laws to master a normal incidence transmission in the material. However, in practice, it is not applicable to industrial controls for two reasons. First, as a single element is used at each transmission, the amplitude level of the surface echo is much lower than that obtained by transmitting with the full array (see Figs. 1a and 4a) and times of flight may be difficult to be measured. Second, the large number of transmissions (43 in the present case) may dramatically decreases inspection rates compare to a conventional paintbrush acquisition mode.
In the next part, a new algorithm is proposed. In particular, it is shown that the optimal delay laws can be found using a small number of transmissions.

3. Generalization of the adaptive technique: the SAUL method

The SAUL method (acronym for ‘Surface Adaptive ULtrasounds’) is an iterative processing of a conventional paintbrush acquisition. The processing thus begins with the transmission of a plane wave by simultaneously exiting all elements and by recording elementary signals in

parallel with the full array. Next, as described in the previous part, the adaptive delay laws are calculated and used for a second ultrasonic shot.
In the SAUL method, this processing is iterated as many times as necessary, until the incident wave ideally fits the front surface, i.e.: new delays laws are calculated after the second shot and are added to the previous ones; then, the resulting delay laws are applied to a third shot; and so on, until the iterative processing converges. Mathematically, the emission delay applied to element *i* (with $1 \leq i \leq 42$) is calculated as follows:

$$E_i^{(j+1)} = \frac{1}{2}\left[\mathrm{Max}\left(t_i^{(j)}\right) - t_i^{(j)} \right] + E_i^{(j)}, \tag{3a}$$

$$E_i^{(j+1)} = E_i^{(j+1)} - \mathrm{Min}\left(E_i^{(j+1)}\right), \tag{3b}$$

where *j* (*j* = 1, 2,…) denotes the shot number in the iterative processing (*j* = 1 corresponds to the first transmission without delay law, i.e. $E_i^{(j)} = 0$ for $j = 1 \ \forall i$). Eq. (3a) expresses the accumulation of delay laws iteration after iteration, while Eq. (3b) is an offset correction ensuring that the minimum delay in the accumulated delay law is still zero. At reception, the delays are simply defined as:

$$R_i^{(j+1)} = \mathrm{Max}\left(E_i^{(j+1)}\right) - E_i^{(j+1)} \tag{4}$$

For an optimal implementation in electronic systems, it is more convenient to express $E_i^{(j+1)}$ and $R_i^{(j+1)}$ only with delays related to previous shot *j*. Substitution of Eq (3a) into Eq. (3b) yields to the following expression of the emission delays

$$E_i^{(j+1)} = E_i^{(j)} - \frac{t_i^{(j)}}{2} - \mathrm{Min}\left(E_i^{(j)} - \frac{t_i^{(j)}}{2} \right). \tag{5}$$

Next, substituting Eq. (5) into Eq.(4), the reception delays may be expressed as

$$R_i^{(j+1)} = \mathrm{Max}\left(E_i^{(j)} - \frac{t_i^{(j)}}{2} \right) - \left(E_i^{(j-1)} - \frac{t_i^{(j)}}{2} \right). \tag{6}$$

Eqs. (5) and (6) are those implemented in the MultiX systems to optimize inspection rates. Fig. 5 presents the emission laws ($E_i^{(1)}$, $E_i^{(2)}$ $E_i^{(3)}$ and $E_i^{(4)}$) calculated with Eq. (5) and applied to the first four shots. For each shot, the recorded B-scan is displayed in Fig. 6. The experimental set-up is unchanged compared to the previous part.

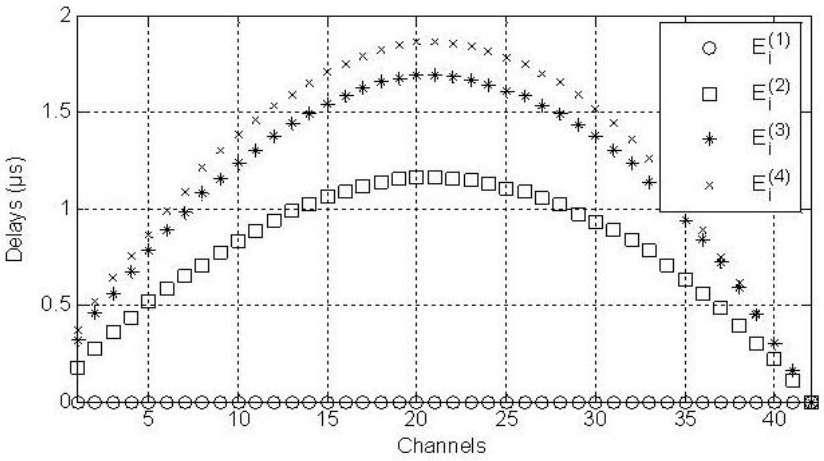

Figure 5: Successive emission delay laws applied in the iterative processing.

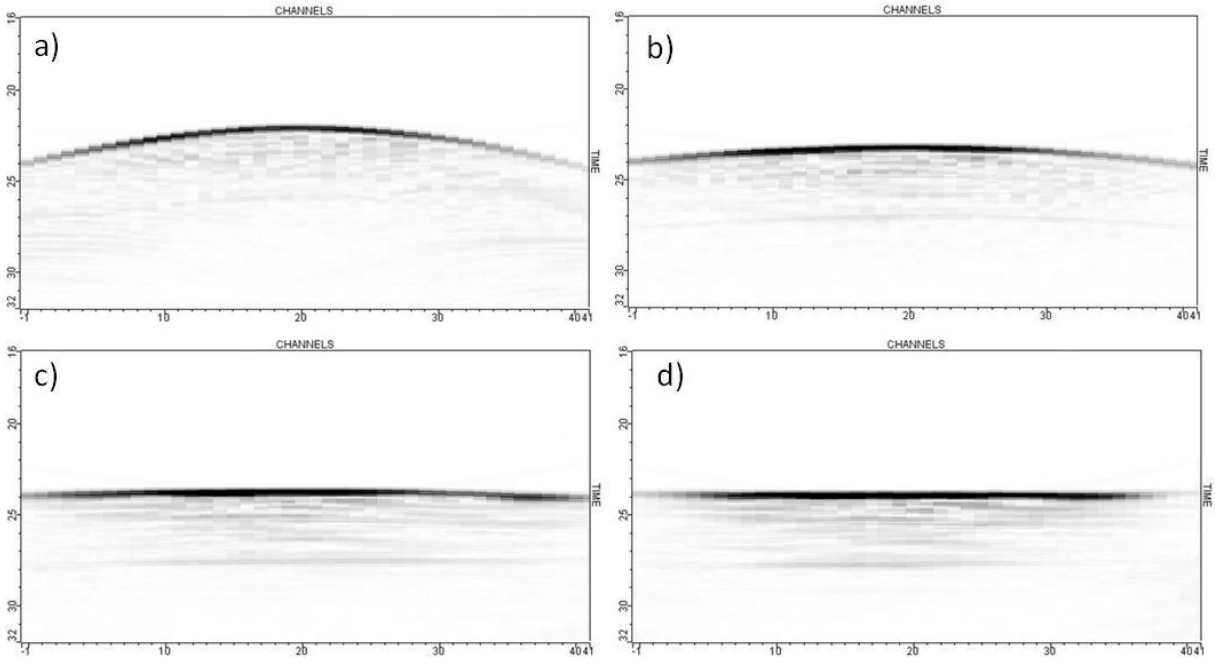

Figure 6: B-scans obtained for the successive shots of the iterative processing: first shot by applying $E_i^{(1)}$ (a); second shot by applying $E_i^{(2)}$ (b); third shot by applying $E_i^{(3)}$ (c); fourth shot by applying $E_i^{(4)}$ (d).

Fig. 5 shows that the iterative processing converges towards the delay law calculated with an electronic scanning at emission (the fourth delay law $E_i^{(4)}$ is identical to that plotted in Fig. 4c). The four B-scans in Fig. 6 illustrate the gradual adaptation of the incident wave to the front surface of the corner radius. Iteration after iteration, the amplitude levels of the front and back surface echoes gradually increase, and the received elementary signals progressively become time coherent. At convergence (Fig. 6d), the Bscan is identical to that provided by an electronic scanning at emission (Fig. 4d).

In a general way, the SAUL algorithm allows to master a normal incidence transmission through any complex surface using a small number of ultrasonic shots (no more 4 or 5 shots are needed). In Fig. 7, a phased array (with 48 elements, 5 MHz central frequency, and 0.6 mm pitch) has been placed in front of the back surface (i.e. the concave surface of the corner radius). The SAUL algorithm then requires 5 shots to achieve convergence. This geometry type is the most unfavorable but the algorithm still converges. Another example is presented in Fig. 8. The probe (with 128 elements and the same characteristic than the previous one) is placed over the shoulder geometry of a composite stiffener, and the SAUL algorithm only requires 3 shots to adapt the incident wave to the surface.

In conclusion of this part, it is important to note that this algorithm is unchanged for linear or matrix probes.

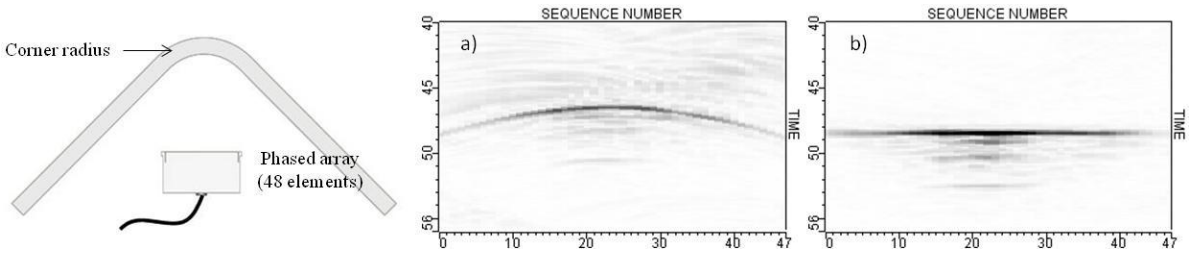

Figure 7: B-scans without processing (a) and by applying the SAUL algorithm with 5 shots (b).

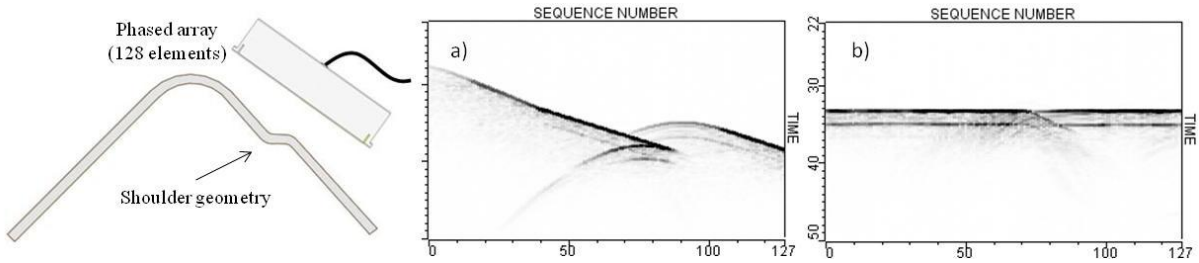

Figure 8: B-scans without processing (a) and by applying the SAUL algorithm with 3 shots (b).

4. Real-time SAUL processing

The SAUL hardware design in MultiX systems enables real-time inspections at high speed: using a phased array of 48 elements and 4 shots in each cycle of iterations, the processing can be enabled with a cycle rate of 400 Hz. Fig. 9 gives an example of acquisition result obtained with the corner radius in Fig. 1a. This component presents a flat bottom hole at mid-length. A linear array of 5 MHz central frequency is placed over the convex part and translated to a length of 280 mm. The probe is composed of 48 elements of 0.5x8 mm², with 0.6 mm pitch. The acquisition has been performed with a cycle of 4 shots, at a speed of 100 mm/s, and data are recorded in 2 mm steps.
At reception, an electric scanning with a sub-aperture of 4 adjacent elements and a scanning step of 1 element has been used (which corresponds to 45 sequences at reception). For each scanning step, the mean of 4 elementary signals is calculated and represented in the form of an electronic B-scan (sequence/time).

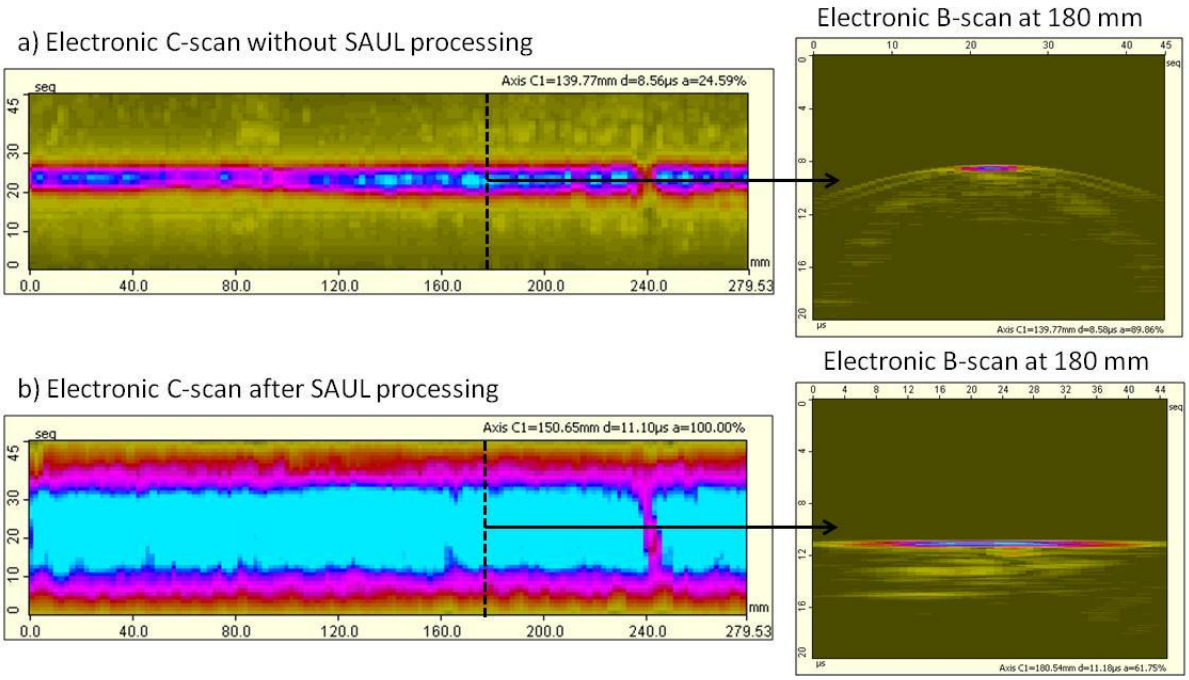

Figure 9: Electronic C-scans without processing (a) and by applying the SAUL function with 4 shots in each cycle of iterations (b).

The electronic C-scans (position/sequence) in Fig. 9 result from the concatenation of the electronic B-scans recorded at each acquisition step. Comparing the two C-scans reveals a larger surface echo when the SAUL processing is enabled. This is mainly due to the time coherence

of elementary signals rather than an increase in their amplitude. This surface echo is large enough to enable triggering during scanning and eliminate water path variations. Then, as presented in Fig. 10, an image of the defect may be obtained by setting an acquisition gate at a given inspection depth in the material.

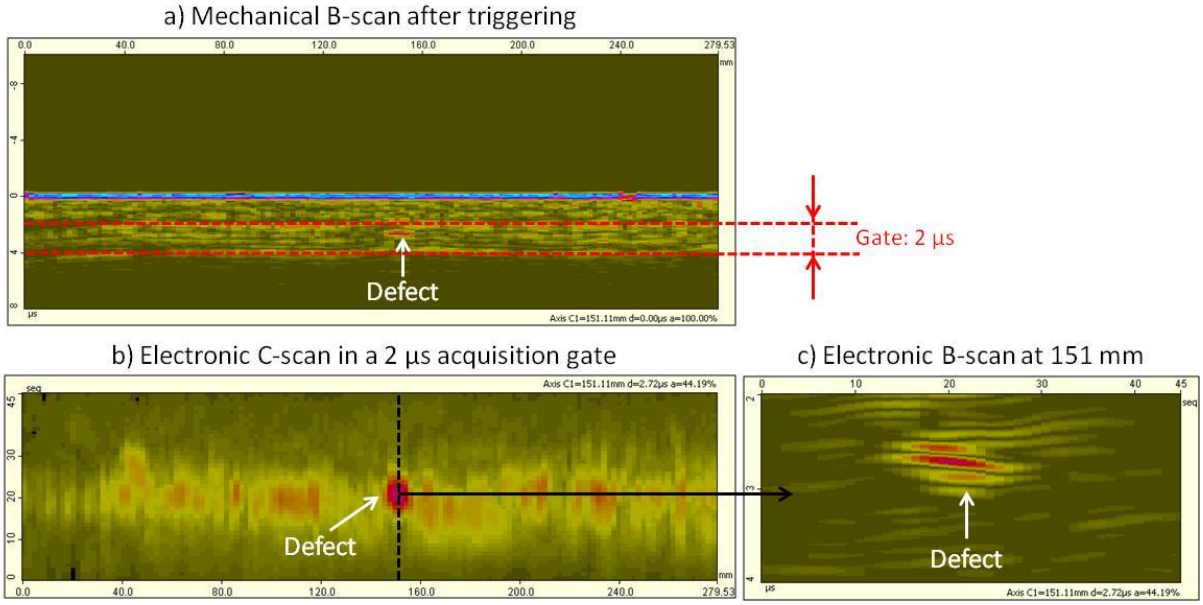

Figure 10: Mechanical B-scan after triggering for the 19th sequence (a); electronic C-scan with a 2 µs acquisition gate (b); electronic B-scan at the defect position (c).

The mechanical B-scan (position/time) in Fig. 10a represents the evolution of a single sequence (i.e. the mean of 4 received elementary signals at the 19th sequence) as function of the probe position. It can be seen that the time of flight of the surface echo is constant and equal to zero due to the triggering applied to each sequence. This compensation of water path variations is essential to set an acquisition gate that does not involve a part of the surface echo (this echo is large and could hide a defect one). In the present configuration, a 2 µs acquisition gate located at 3 µs from the surface echo is optimal. The new electronic C-scan displayed in Fig. 10b now highlights the defect echo with an acceptable signal-to-noise ratio.

It should be noted that the C-scan image does not allow to characterize the defect (i.e., dimensions, depth...) with accuracy because the exact geometry and/or the position of the corner radius are not assumed to be known in practice, as in the present experiment. New developments are in progress to build true C-scan images from the SAUL algorithm and a better characterization is expected soon [10].

4. Conclusions

In this paper, a new adaptive inspection technique implemented in MultiX systems has been presented. This technique is based on an iterative processing of a paintbrush acquisition mode and requires only a small number of ultrasonic shots to master a normal incidence transmission through a complex surface of a composite structure. All different parts (flat, concave or convex surfaces) of a given component can be inspected using a same transducer array, such as a conventional probe with a flat active aperture. An acquisition result performed with a corner radius has been presented and shows that the SAUL method is promising in terms of scanning rate and detection ability. Future works will focus on the geometry reconstruction from the SAUL algorithm in order to improve the defect characterization.

References

[1] R. D. Adams, P. Cawley, 'A review of Defect Types and Nondestructive Testing Techniques for Composites and Bonded Joints', NDT International, Vol 21, No 4, pp. 208-222, August 1988.

[2] G. Ithurralde, 'Advanced Functions of PAUT (Phased Arrays for Ultrasound Testing) in Aeronautics', ECNDT Proceeding, Berlin, September 2006.

[3] N. Dominguez, G. Ithurralde, 'Ultra-fast Ultrasonic Inspection for Aeronautical Composites using Paintbrush Acquisitions and Data Processing on GPU', European Conference on NDT, Moscow, 2010.

[4] R. Meier, J. Becker, T. Rehfeld, Method for the Ultrasonic Testing of a Workpiece within a Curved Region of its Surface and Device Suitable for the Execution of the Process, Patent No US 7516664 B2, April 2009.

[5] F. D. Young, C. T. Uyehara, Hien T. Bui, 'Ultrasonic Testing of Corner Radii Having Different Angles and Sizes, Patent No US2009/0211361 A1, August 2009.

[6] A. Maurer, W. Haase, W. De Odorico, 'Phased Array Application in Industrial Scanning Systems', ECNDT Proceeding, September 2006.

[7] A. Maurer, M. Strauss, W. De Odorico, 'Roman Koch, Method and Circuit Arrangement for Disturbance-Free Examination of Objects by Means of Ultrasonic Waves', Patent No US2006/0195273 A1, August 2006.

[8] S. Robert, O. Casula, M. Njiki, O. Roy, 'Assessment of Real-Time Techniques for Ultrasonic Nondestructive Testing', Review of Progress in QNDE, in press, 2012.

[9] S. Robert, O. Casula, A. Nadim, 'Procédé de Commande de Transducteurs d'une Sonde à Ultrasons, Programme d'Ordinateur et Dispositif de Sondage par Ultrasons', France Patent No FR 10/56217, July 2010.

[10] S. Robert, O. Casula, E. Iakovleva, 'Procédé de Détermination d'une Surface d'un Objet par Sondage Echographique, Programme d'Ordinateur Correspondant et Dispositif de Sondage à Ultrasons', France Patent No FR 11/60399, November 2011.